Electronic Supplementary Material (ESI) for Materials Chemistry Frontiers.

Supporting Information

Hypersonic Poration of Supported Lipid Bilayers

Yao Lu[1,2], Jurriaan Huskens[2,] Wei Pang[1], Xuexin Duan[1,]**

[1.] State Key Laboratory of Precision Measuring Technology & Instruments, Tianjin University, Tianjin 300072, China.

[2.] Molecular Nanofabrication group, MESA+ Institute for Nanotechnology, University of Twente, 7500 AE, Enschede, The Netherlands.

* E-mail: j.huskens@utwente.nl, xduan@tju.edu.cn.

1. Microfabrication process of the integrated microchip.

Figure S1 shows the microfabrication process of the integrated microchip compose of a bulk acoustic wave (BAW) resonator and a gold electrode. During fabrication, the relative spatial structure of the top/bottom electrode and the piezoelectric layer will generate parasitic capacitance and/or inductance. When the resonator vibrates at longitudinal mode, the parasitic capacitance and/or inductance would generate a new vibrating mode, which will decrease the quality factor of the device and affect the detection the main working mode. Thus, we tried to optimize the shape the resonator and found that the parasitic effect would be minimized with the polygonal shape.

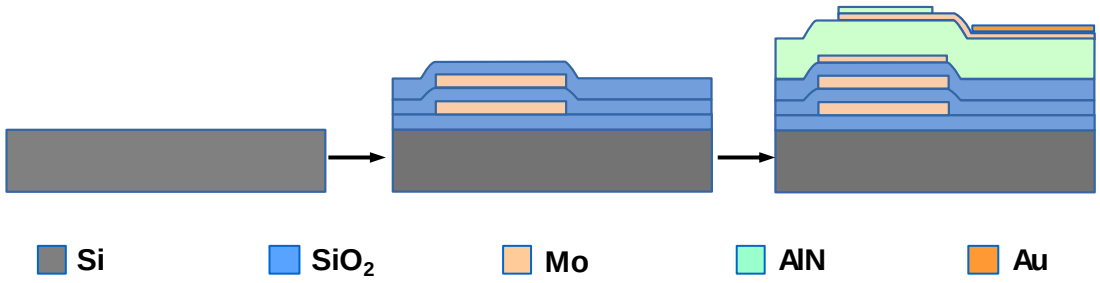

Figure S1. Microfabrication process of the integrated microchip.

2. Fluorescence measurements of the supported lipid bilayer.

Figure S2 shows fluorescence imaging of the supported lipid bilayer (SLB) made of N-(7-Nitrobenz-2-Oxa-1,3-Diazol-4-yl)-1,2-Dihexadecanoyl-sn-Glycero-3-Phosphoethanolamine (NBD-PE), which performs uniform green fluorescence with an integrated membrane.

In Video S1-S3, the fluorescent SLB was also made of NBD-PE to facilitate the fluorescence imaging of the changes of SLB under hypersound.

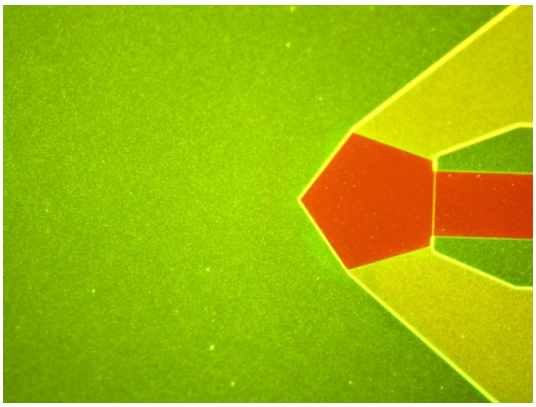

Figure S2. Fluorescence imaging of the SLB made of NBD-PE on top of the resonator.

3. Simulations of the NEMS resonator.

To understand the mechanism of membrane deformation induced by the propagation of hypersound, we used a 2D finite element model (FEM) simulation. Figure S3 shows the simulated patterns of the deformation of the resonator. The corresponding vertical displacements of the resonator surface under hypersound of different input powers are illustrated in Table S1.

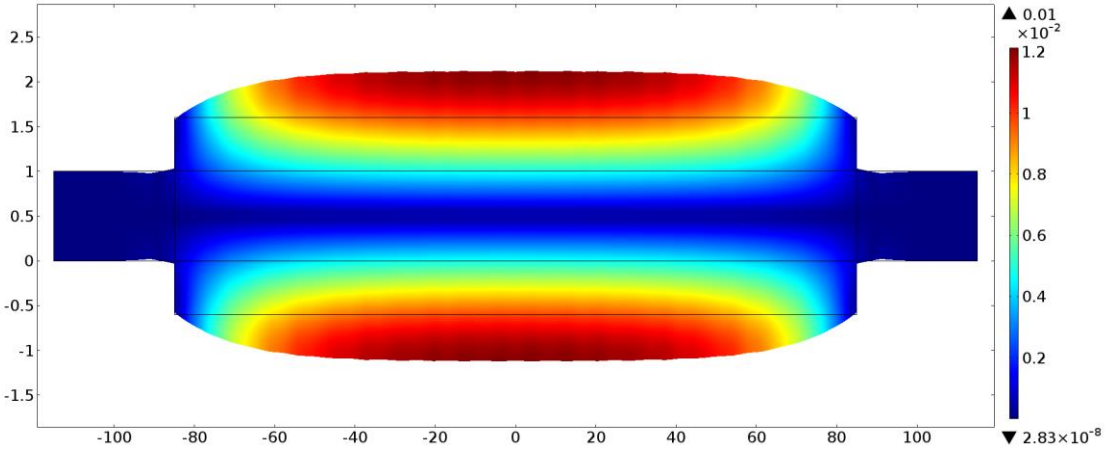

Figure S3. FEM simulations of the surface deformation when hypersound is activated from the resonator. The frequency of the resonator was 1.6 GHz and the input power of hypersound was 500 mW. The color bar indicates the vertical displacement of the resonator surface during the propagation of hypersound from min (blue) to max (red).

Table S1. The vertical displacements of the resonator surface at hypersound of different input powers.

Power (mW)	Vertical Displacement (nm)
3.2	0.407
10	0.719
20	1.02
50	1.61
100	2.27
200	3.21
300	3.94
400	4.55
500	5.08

4. CV tests of the SLB.

As Figure S4 shows, CV curves were recorded with the SLB-coated gold electrode by switching on and off the hypersound of different powers and durations. In the case of 250 mW for 5 min, the curve recovered to the original state by turning off hypersound (blue dash line). However, when the input power of hypersound was increased to 500 mW and the stimulation time was extended to 30 min, the curve did not recover any more (purple dash line) after turning of hypersound, which indicates that the SLB has been damaged under such high stimulation.

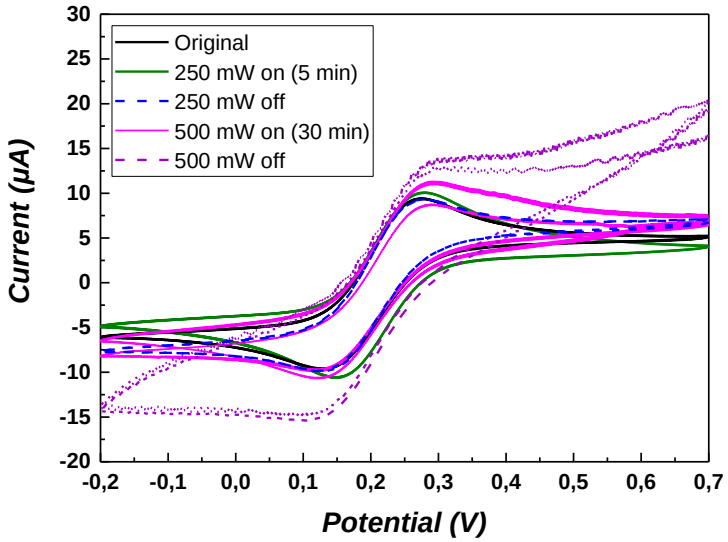

Figure S4. Real-time CV responses of 1 mM $K_3Fe(CN)_6$ in 1 M KCl at SLB by switching on and off the hypersound of different input powers and durations.

5. Electrical measurements of the SLB.

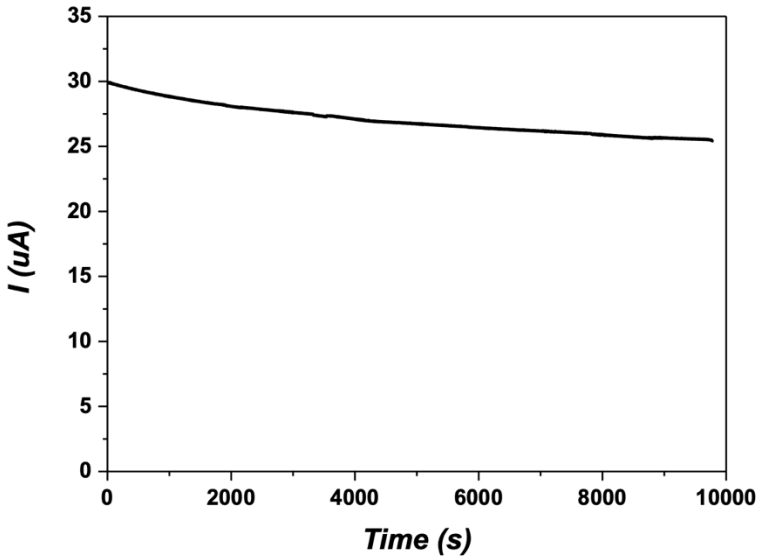

Figure S5. Real-time detection of ion current on the gold electrode without SLB while switching on and off the hypersound.

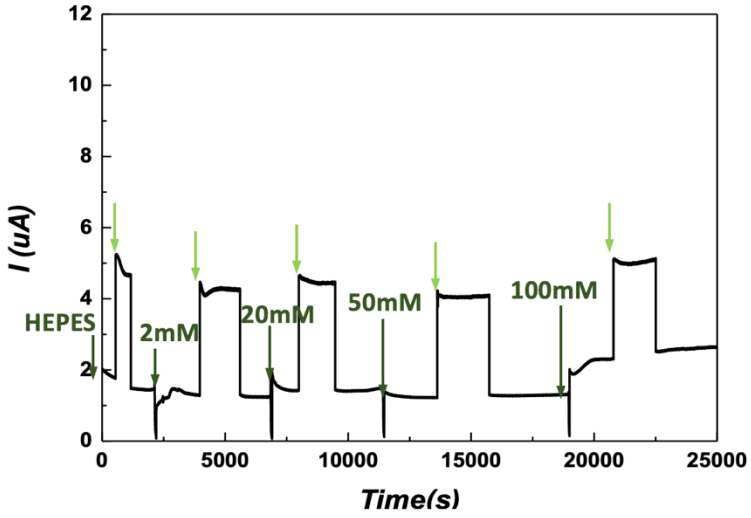

Figure S6. Real-time detection of ion current through the SLB in KCl solutions of different concentrations by switching on (green arrows) and off the hypersound. The concentrations of the KCl solutions were, successively, 2, 20, 50 and 100 mM.

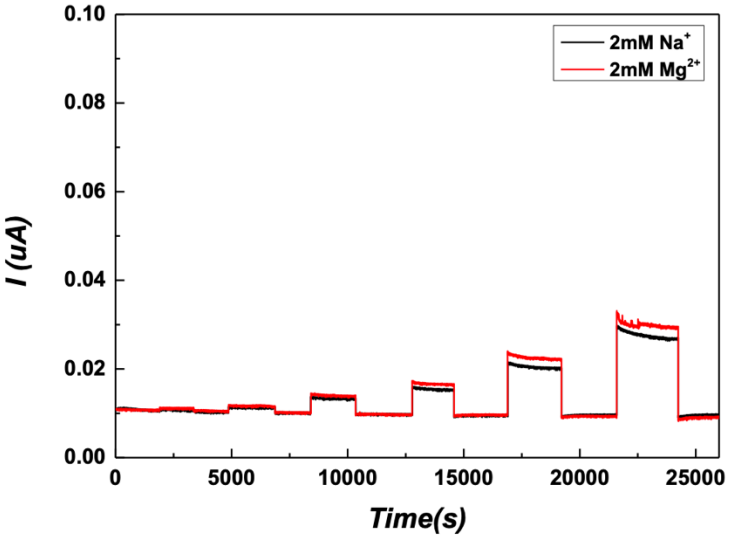

Figure S7. Real-time recordings of the ion current through the SLB on the integrated device by alternatingly switching on and off the hypersound (the input powers were successively 10, 32, 50, 100, 160, 250 mW). The electrolyte solutions were respectively NaCl, $MgCl_2$ (2 mM in pure water).